European Spine Journal (2020) 29:840–848
https://doi.org/10.1007/s00586-020-06312-y

ORIGINAL ARTICLE

Check for updates

Thoracic kyphosis and pelvic anteversion in patients with adult spinal deformity increase while walking: analyses of dynamic alignment change using a three-dimensional gait motion analysis system

Kousei Miura[1,2] · Hideki Kadone[3] · Masao Koda[1] · Tetsuya Abe[1] · Toru Funayama[1] · Hiroshi Noguchi[1] · Kentaro Mataki[1] · Katsuya Nagashima[1] · Hiroshi Kumagai[1] · Yosuke Shibao[1] · Kenji Suzuki[4] · Masashi Yamazaki[1]

Received: 9 January 2019 / Revised: 4 August 2019 / Accepted: 18 January 2020 / Published online: 31 January 2020
© Springer-Verlag GmbH Germany, part of Springer Nature 2020

Abstract

Purpose To determine dynamic changes of spinopelvic alignment while walking using a three-dimensional (3D) gait motion analysis in adult spinal deformity (ASD) patients.

Methods This study included 20 ASD patients. The 3D gait motion analysis (Vicon) was performed during continuous walking to their limit. Dynamic parameters were obtained using reflective markers on the spinous processes, which were segmented into thoracic (T-), lumbar (L-), and whole spine (S-), sagittal spinal distance (SVA) and coronal one (CVA), sagittal spinal angle to the vertical axis (SA) and coronal one (CA), sagittal pelvic angle to the horizontal axis (P-SA) and coronal (P-CA), and thoracic limited spinal angle to the pelvic angle (T-P SA) and lumbar one (L-P SA). The dynamic variables at the final lap were compared with those at the first lap of an oval walkway.

Results Spinal kyphotic deformity deteriorated significantly. As for pelvic angle, the mean P-SA parameters (first lap/final lap) were 3.2°/5.2°. Anteversion of pelvic sagittal angle increased significantly after continuous walking to their limit. In particular, regarding limited spinal angle to the pelvic angle, the mean T-P SA parameters were 30.5°/36.2° and L-P SA parameters were 6.4°/6.8°. Thoracic kyphotic angle increased significantly, but lumbar kyphotic angle did not change.

Conclusion Decrease of thoracic kyphosis and pelvic retroversion has been recognized as a compensation for ASD on standing radiograph. Our 3D gait motion analysis to determine spinal balance found thoracic kyphosis and pelvic anteversion increased significantly in patients with ASD after continuous walking to the limit of their endurance until they were fatigued, indicating a failure of compensation for ASD.

Graphic abstract

These slides can be retrieved under Electronic Supplementary Material.

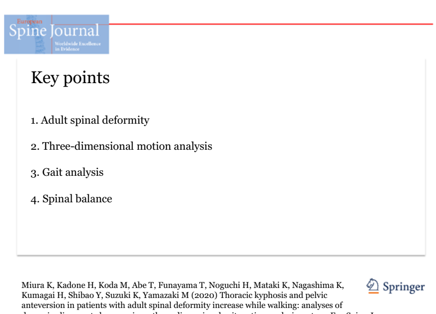

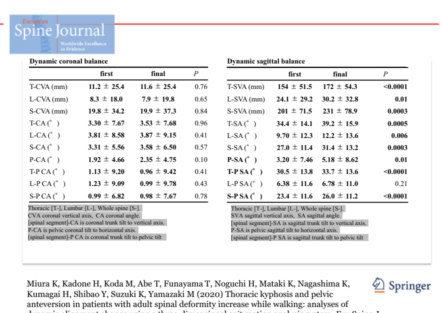

Dynamic coronal balance

	first	final	P
T-CVA (mm)	11.2 ± 25.4	11.6 ± 25.4	0.76
L-CVA (mm)	8.3 ± 18.0	7.9 ± 19.8	0.65
S-CVA (mm)	19.8 ± 34.2	19.9 ± 37.3	0.84
T-CA (°)	3.30 ± 7.67	3.53 ± 7.68	0.96
L-CA (°)	3.81 ± 8.58	3.87 ± 9.15	0.41
S-CA (°)	3.31 ± 5.56	3.58 ± 6.50	0.57
P-CA (°)	1.92 ± 4.66	2.35 ± 4.75	0.10
T-P CA (°)	1.13 ± 9.20	0.96 ± 9.42	0.41
L-P CA (°)	1.23 ± 9.09	0.99 ± 9.78	0.43
S-P CA (°)	0.99 ± 6.82	0.98 ± 7.67	0.78

Thoracic [T-], Lumbar [L-], Whole spine [S-].
CVA coronal vertical axis, CA coronal angle.
[spinal segment]-CA is coronal trunk tilt to vertical axis.
P-CA is pelvic coronal tilt to horizontal axis.
[spinal segment]-P CA is coronal trunk tilt to pelvic tilt

Dynamic sagittal balance

	first	final	P
T-SVA (mm)	154 ± 51.5	172 ± 54.3	<0.0001
L-SVA (mm)	24.1 ± 29.2	30.2 ± 32.8	0.01
S-SVA (mm)	201 ± 71.5	231 ± 78.9	0.0003
T-SA (°)	34.4 ± 14.1	39.2 ± 15.9	0.0005
L-SA (°)	9.70 ± 12.3	12.2 ± 13.6	0.006
S-SA (°)	27.0 ± 11.4	31.4 ± 13.2	0.0003
P-SA (°)	3.20 ± 7.46	5.18 ± 8.62	0.01
T-P SA (°)	30.5 ± 13.8	33.7 ± 13.6	<0.0001
L-P SA (°)	6.38 ± 11.6	6.78 ± 11.0	0.21
S-P SA (°)	23.4 ± 11.6	26.0 ± 11.2	<0.0001

Thoracic [T-], Lumbar [L-], Whole spine [S-].
SVA sagittal vertical axis, SA sagittal angle.
[spinal segment]-SA is sagittal trunk tilt to vertical axis.
P-SA is pelvic sagittal tilt to horizontal axis.
[spinal segment]-P SA is sagittal trunk tilt to pelvic tilt

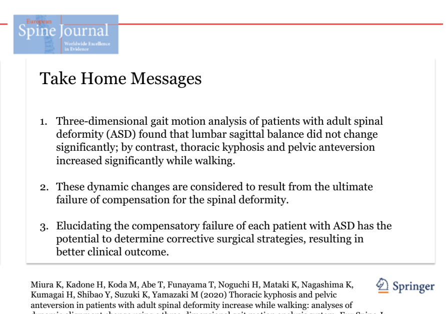

Keywords Adult spinal deformity · Three-dimensional motion analysis · Gait analysis · Spinal balance

Electronic supplementary material The online version of this article (https://doi.org/10.1007/s00586-020-06312-y) contains supplementary material, which is available to authorized users.

Extended author information available on the last page of the article

Introduction

To date, spinopelvic parameters measured using conventional whole-spine radiographs with the patient in a standing position are widely used as the criterion standard for diagnosis, as prognostic values, and as surrogate outcome measures after surgery in patients with adult spinal deformity (ASD). Various studies have found that sagittal spinopelvic misalignment seen on standing radiographs causes pain and deteriorates health-related quality of life [1–8]. However, we often encounter patients whose symptoms and posture deteriorate while walking, suggesting that the pathology of ASD includes a dynamic factor as a result of their deformity. Moreover, calculating sagittal spinal parameters measured using conventional whole-spine radiograph is poorly reproducible. The sagittal vertical axis and the pelvic tilt are affected by the patient's position [9]. Static evaluation alone might not be sufficient to understand the pathology of ASD fully, and we consider dynamic alignment change is clinically important. To resolve these shortcomings, we performed three-dimensional (3D) gait analysis to determine dynamic change of spinal alignment. With recent advances, 3D gait motion capture analysis has been applied to detailed analysis of healthy subjects and trials for analysis of various kinds of spinal deformity including dropped head syndrome, iatrogenic flatback syndrome, and ankylosing spondylitis [10–13]. The purpose of the present study was to determine the dynamic change of spinopelvic alignment using 3D gait motion analysis system while patients with ASD walked to the limit of their endurance.

Materials and methods

Participants

The radiographic inclusion criteria were as follows: pelvic incidence minus lumbar lordosis (PI—LL) > 10°; sagittal vertical axis (SVA) > 4 cm; and pelvic tilt (PT) > 20°, as parameters defining global sagittal misalignment according to the SRS-Schwab ASD Classification [6]. Patients who were unable to walk without assistance were excluded from the present series. The present study included 20 patients (3 male and 17 female) who underwent 3D gait analysis for ASD. The mean of age of the patients was 70 years (range 55–79 years), mean height was 148 cm (range 131–163 cm), and mean weight was 53 kg (range 39–76 kg) (Table 1). The present study was performed in accordance with the contemporary amendments of the Declaration of Helsinki and within an appropriate ethical framework. The study design was approved by the ethics committee of our institute. Written informed consent was obtained from all patients included in this study.

Table 1 Demographic data ($n = 20$)

	Mean	Range
Age (years)	70	55 to 79
Height (cm)	148	131 to 163
Weight (kg)	53	39 to 76
SVA (mm)	142	70 to 197
TK (°)	22	− 5 to 57
LL (°)	1.8	− 33 to 38
PT (°)	38	21 to 63
PI (°)	48	18 to 62
TPA (°)	43	24 to 64

SVA sagittal vertical axis, *TK* thoracic kyphosis, *LL* lumbar lordosis, *PT* pelvic tilt, *PI* pelvic incidence, *TPA* T1 pelvic angle

Radiological assessments (static evaluation)

We evaluated whole spinal radiographs taken with the patient in a standing position before 3D gait motion analysis. Each patient was asked to stand comfortably with their hands placed on their clavicles. Static spinal parameters were evaluated as follows: sagittal vertical axis (SVA); thoracic kyphosis (TK); lumbar lordosis (LL); pelvic tilt (PT); pelvic incidence (PI); T1 pelvic angle (TPA); coronal Cobb angle of the thoracolumbar and lumbar scoliosis (Cobb); and coronal balance (C7-CSVL, the distance between C7 plumb line and the center sacral vertical line) (Fig. 1).

Three-dimensional gait motion analysis (dynamic evaluation)

Three-dimensional motion analysis was performed using a Vicon MX system (Vicon, Oxford, UK) comprising 16 cameras and 38 reflective markers variously attached on the head, spinal spinous processes, pelvis, and upper and lower limbs of the patients. The 3D gait analysis was performed in a laboratory room set up to measure gait, which contained an oval walkway comprising two parallel 10 m straight paths and two semicircular paths of approximately 1 m radius (Fig. 2). Each patient was asked to walk continuously for as long as possible at a comfortable pace (to the limit of their endurance until they were fatigued) on the oval walkway.

Outcome measures and statistical analyses

Obtained dynamic spinal parameters were defined as follows: thoracic SVA and thoracic CVA (T-SVA and T-CVA, the sagittal and coronal distance between reflective markers on the C7 and T12 spinous processes); thoracic SA and thoracic CA (T-SA and T-CA, the sagittal and coronal angle between the vertical axis and the line connecting the

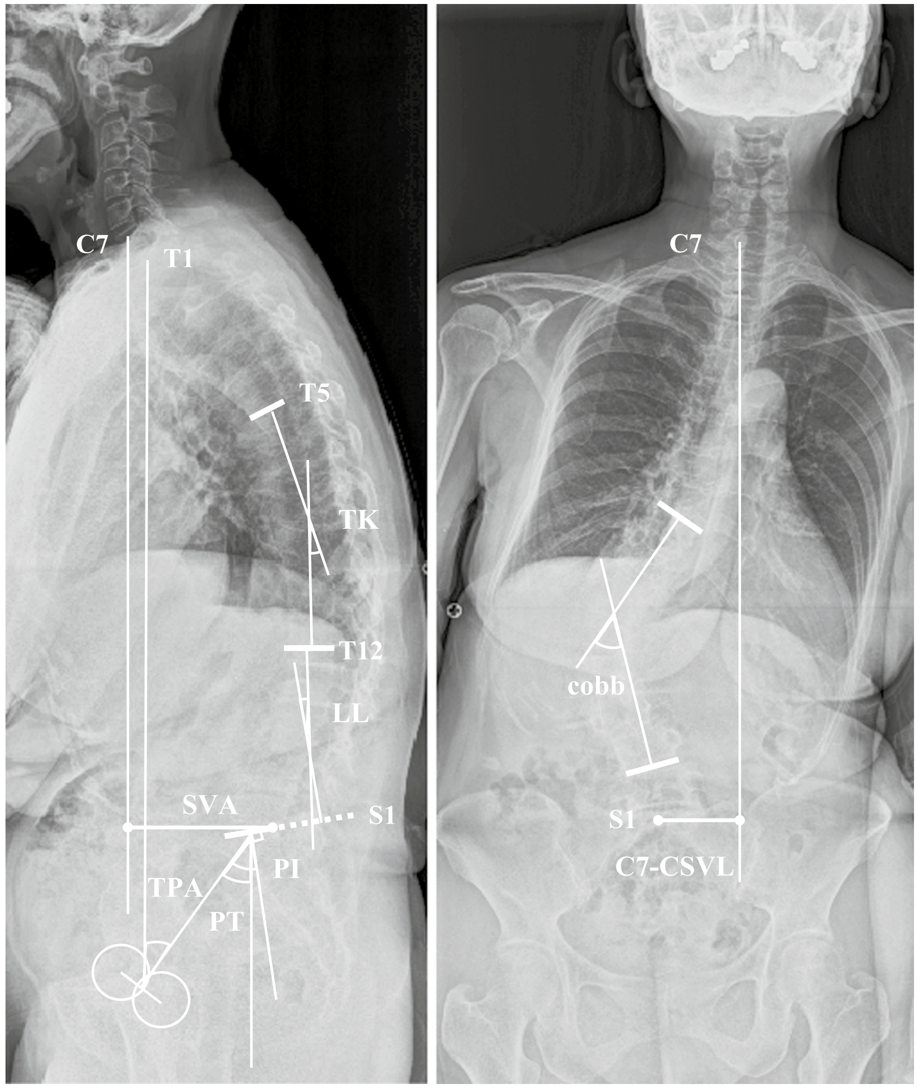

Fig. 1 Representation of measured static spinal parameters. *SVA* the sagittal vertical axis, *TK* thoracic kyphosis (T5-12), *LL* lumbar lordosis (T12-S1), *PT* pelvic tilt, *PI* pelvic incidence, *TPA* T1 pelvic angle, *Cobb* coronal Cobb angle of the thoracolumbar and lumbar scoliosis, and *C7-CSVL* the distance between C7 plumb line and the center sacral vertical line

reflective markers on C7 and T12 spinous processes); lumbar SVA and lumbar CVA (L-SVA and CVA, the sagittal and coronal distance between reflective markers on the T12 and S1 spinous processes); lumbar SA and lumbar CA (L-SA and L-CA, the sagittal and coronal angle between the vertical axis and the line connecting the reflective markers on T12 and S1 spinous processes); whole-spine SVA (S-SVA, the sagittal distance between reflective markers on the C7 and S1 spinous processes); whole-spine SA (S-SA, the angle between the vertical axis and the line connecting the reflective markers on C7 and S1 spinous processes); and pelvic sagittal and coronal angle (P-SA and P-CA, the sagittal and coronal angle between the horizontal axis and the line connecting the reflective markers on the anterior superior iliac spine (ASIS) and the posterior superior iliac spine (PSIS)) (Fig. 3).

Additionally, we evaluated the dynamic parameters of trunk tilt considering pelvic angle. They were defined as follows: thoracic–pelvic sagittal angle and coronal angle (T-P SA and T-P CA, the sagittal and coronal angle between the line connecting the reflective markers on the C7 and T12 spinous process and the line connecting the reflective markers on the ASIS and PSIS); lumbar–pelvic sagittal angle and coronal angle (L-P SA and L-P CA, the sagittal and coronal angle between the line connecting the reflective markers on T12 and S1 spinous process and the line connecting the reflective markers on the ASIS and PSIS); and whole-spine–pelvic sagittal angle and coronal angle (S-P SA and S-P CA, the sagittal and coronal angle between the line connecting the reflective markers on C7 and S1 spinous process and the line connecting the reflective markers on the ASIS and PSIS).

We compared these dynamic variables between at the first lap and at the final lap of the oval walkway using a Wilcoxon signed-rank test. A Spearman correlation coefficient was used to analyze the relationship between the variations

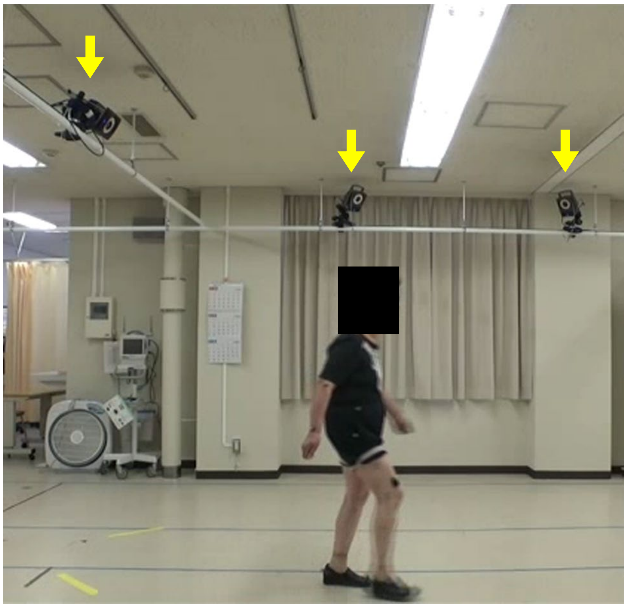

Fig. 2 3D gait motion analysis was performed using a Vicon MX system (Vicon, Oxford, UK), comprising 16 cameras set up to measure gait (arrows) in a laboratory, which has an oval walkway comprising two parallel 10 m straight paths and two semicircular paths of approximately 1 m radius. It is possible to analyze continuous long distance walking on a flat surface

in dynamic spinal parameters with significant change while walking and the static spinal parameters evaluated using the whole-spine radiograph for definition of the global sagittal misalignment (SVA, PI minus LL, PT). All statistical analyses were conducted using the JMP software package, version 14.0.0 (SAS Institute Inc., Cary, NC, USA). $P < 0.05$ was considered significant for tests of statistical inference.

Results

Radiological assessments (static evaluation)

The mean values for each radiological spinal parameter were as follows: SVA, 142 ± 43 mm (range 70–197 mm); TK, 22° ± 17° (range −5° to 57°); LL, 1.8° ± 17° (range −33° to 38°); PT, 38° ± 12° (range 21°–63°); PI, 48° ± 11° (range 18°–62°); TPA, 43° ± 12° (range 24°–64°); Cobb, 20° ± 16° (range 1°–49°); and C7CSVL, 12 ± 23 mm (range −29 to 68 mm).

Three-dimensional gait motion analysis (dynamic evaluation)

Dynamic spinal parameters for coronal balance are summarized in Table 2. The mean T-CVA, L-CVA, and S-CVA were 11.2 ± 25.4 mm, 8.28 ± 18.0 mm, and 19.8° ± 34.2 mm, respectively, at the first lap, and 11.6 ± 25.7 mm, 7.93 ± 19.8 mm, and 19.9 ± 37.3 mm, respectively, at the final lap. The mean T-CA, L-CA, and S-CA were 3.3° ± 7.7°, 3.8° ± 8.6°, and 3.3° ± 5.5°, respectively, at the first lap, and 3.5° ± 7.8°, 3.9° ± 9.2°, and 3.6° ± 6.5°, respectively, at the final lap. The mean P-CA was 2.0° ± 4.7° at the first lap, and 2.3° ± 4.7° at the final lap. The mean T-P CA, L-P CA, and S-P CA were 1.1° ± 9.2°, 1.2 ± 9.0°, and 1.0° ± 6.8°, respectively, at the first lap, and −2.5° ± 19.5°, 1.0 °±9.8°, and 1.0° ± 7.7°, respectively, at the final lap. None of the dynamic spinal parameters for coronal balance showed any significant change (Fig. 4).

Dynamic spinal parameters for sagittal balance are summarized in Table 3. The mean T-SVA, L-SVA, and S-SVA

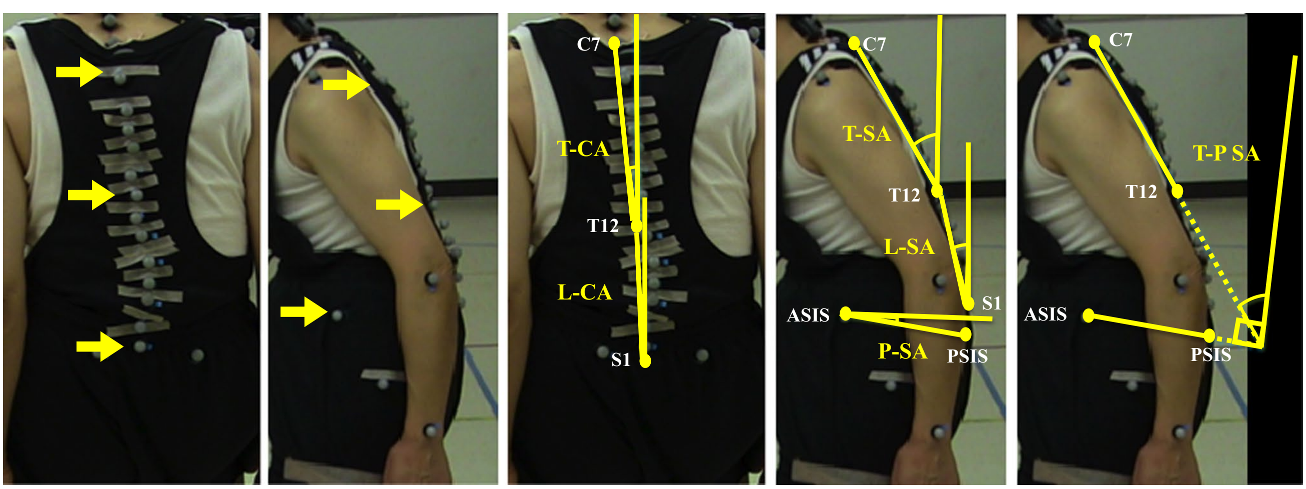

Fig. 3 Reflective markers attached on the spinal spinous processes and pelvis (arrows). This figure shows defined dynamic spinal parameters (CA, SA and PSA, T-P SA). *ASIS* the anterior superior iliac spine, *PSIS* the posterior superior iliac spine, *CA* coronal angle, *SA* sagittal angle, *P-SA* pelvic sagittal angle, and *T-P SA* thoracic–pelvic sagittal angle

were 154 ± 51.5 mm, 24.1 ± 29.2 mm, and 201 ± 71.5 mm, respectively, at the first lap, and 173 ± 54.3 mm, 30.1 ± 32.8 mm, and 231 ± 78.5 mm, respectively, at the final lap. The mean T-SA, L-SA, and S-SA were 34.4° ± 14.1°, 9.7° ± 12.3°, and 27.0° ± 11.4°, respectively, at the first lap, and 39.2° ± 16.0°, 12.2° ± 13.6°, and 31.4° ± 13.2°, respectively, at the final lap. The mean P-SA was 3.2° ± 7.5° at the first lap, and 5.2° ± 8.6° at the final lap. The mean T-P SA, L-P SA, and S-P SA were 30.5° ± 13.8°, 6.4° ± 11.6°, and 23.4° ± 11.6°, respectively, at the first lap, and 36.2° ± 17.9°, 6.8° ± 11.0°, and 26.0° ± 11.2°, respectively, at the final lap. Dynamic sagittal balance and spinal kyphotic deformity deteriorated significantly after patients had walked until they were fatigued. Spinal sagittal angle to the horizontal plane and kyphotic sagittal angle of both the thoracic and lumbar segments increased significantly. Simultaneously, anteversion of the pelvic sagittal angle increased significantly. For this reason, spinal sagittal angle to the pelvic sagittal angle and thoracic kyphotic sagittal angle increased significantly and lumbar kyphotic sagittal angle was not changed (Figs. 5 and 6). There was no significant correlation between the increase in thoracic kyphosis (T-P SA) and the static spinal parameters. Only SVA was positively correlated with the increase of pelvic anteversion (P-SA) ($r = 0.49$, $p = 0.027$). The other static spinal parameters showed no significant correlation with the increase of pelvic anteversion.

Table 2 Dynamic spinal parameters for coronal balance (mean ± SD)

	First	Final	*P*
T-CVA (mm)	11.2 ± 25.4	11.6 ± 25.4	0.76
L-CVA (mm)	8.3 ± 18.0	7.9 ± 19.8	0.65
S-CVA (mm)	19.8 ± 34.2	19.9 ± 37.3	0.84
T-CA (°)	3.30 ± 7.67	3.53 ± 7.68	0.96
L-CA (°)	3.81 ± 8.58	3.87 ± 9.15	0.41
S-CA (°)	3.31 ± 5.56	3.58 ± 6.50	0.57
P-CA (°)	1.92 ± 4.66	2.35 ± 4.75	0.10
T-P CA (°)	1.13 ± 9.20	0.96 ± 9.42	0.41
L-P CA (°)	1.23 ± 9.09	0.99 ± 9.78	0.43
S-P CA (°)	0.99 ± 6.82	0.98 ± 7.67	0.78

Thoracic [T-], Lumbar [L-], Whole spine [S-]. CVA coronal vertical axis, CA coronal angle. [spinal segment]-CA is coronal trunk tilt to vertical axis. P-CA is pelvic coronal tilt to horizontal axis. [spinal segment]-P CA is coronal trunk tilt to pelvic tilt

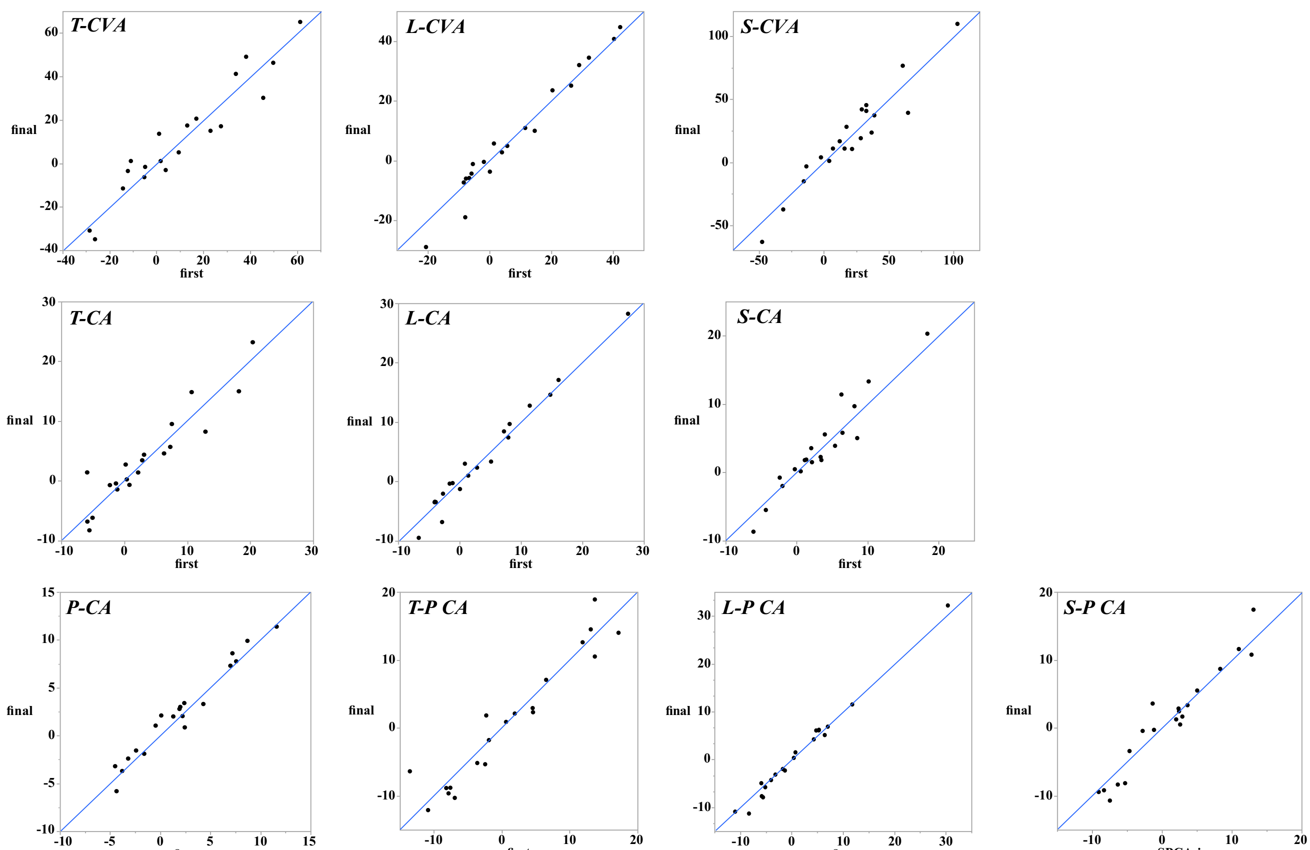

Fig. 4 Plots of dynamic spinal parameters for coronal balance at the final lap vs at the first lap. Blue line shows the *Y* value equals the *X* value. No dynamic spinal parameters for coronal balance showed any significant change

Discussion

In the present study, spinal balance in the sagittal plane alone deteriorated significantly with anterior shift, while patients with global sagittal misalignment walked until they were fatigued. By contrast, coronal spinal balance was not changed. When evaluating global spinal alignment statically using whole-spine radiographs, sagittal spinal misalignment is more important than coronal spinal misalignment [2, 4]. The present study indicated that when spinal balance is evaluated dynamically while the patient is walking, as in the static evaluation, sagittal spinal balance is more important than coronal spinal balance.

All patients showed pelvic retroversion while in a standing position due to compensation for spinal alignment because the inclusion criteria of the present study included PT > 20°. Nevertheless, sagittal pelvic anteversion increased as assessed by the 3D gait motion analysis while patients were walking. Previous studies of 3D gait motion analysis using Vicon have also shown anterior shift of the spinal sagittal vertical axis, decrease of pelvic posterior tilt, and increase of pelvic anteversion [14, 15]. The present finding of attenuation of pelvic retroversion while the patients were walking is consistent with the previous studies. However, dynamic SVA (T-SVA, L-SVA, S-SVA) and SA (T-SA, L-SA, S-SA) evaluated were distance and angle to vertical axis, and so lower limb joint angles and pelvic angle were not sufficiently considered. The lower limb joint angles affect SVA as seen on plain radiographs [16] and should be considered in dynamic evaluations. Therefore, we attempted to evaluate the limited spinal balance by excluding the effect of pelvic and lower limb joint angle by calculating the angles between the line connecting the spinal processes and the pelvic horizontal plane (T-P, L-P, S-P SA, and CA). As a result of the limited spinal balance, thoracic kyphotic sagittal angle (T-P SA) increased significantly, but lumbar kyphotic sagittal angle (L-P SA) was not changed. Decrease of thoracic kyphosis and pelvic retroversion has been recognized as a compensation for the decrease of lumbar lordosis by spinal degenerative change. These compensatory mechanisms allow the patients to improve global spinal alignment and to restore the gravity line position and horizontal gaze.

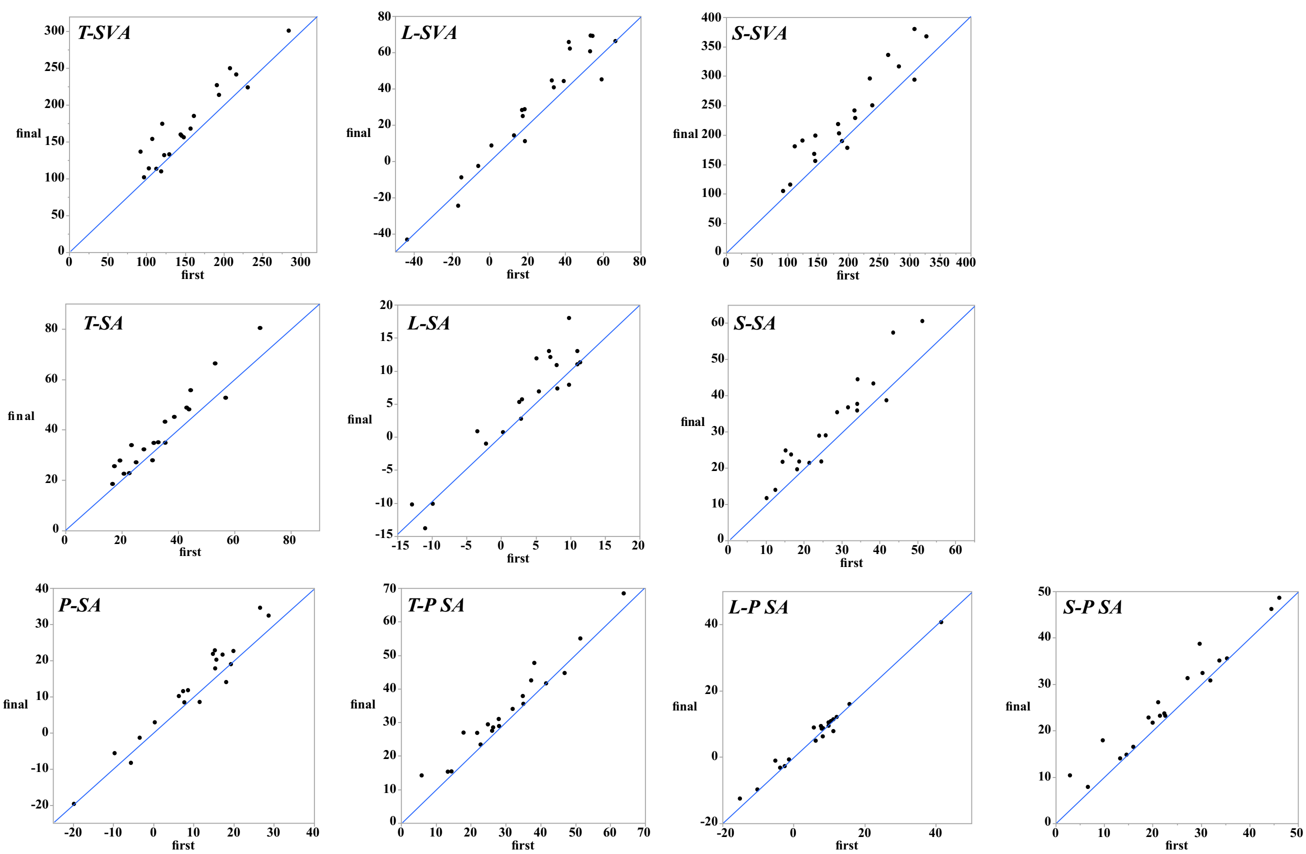

Fig. 5 Plots of dynamic spinal parameters for sagittal balance at the final lap vs at the first lap. Blue line shows the *Y* value equals the *X* value. Spinal kyphotic deformity (T-SVA, L-SVA, S-SVA, T-SA, L-SA, and S-SA) deteriorated significantly, and anteversion of pelvic sagittal angle (P-SA) increased significantly. Spinal sagittal angle to the pelvic sagittal angle and thoracic kyphotic sagittal angle (T-P SA) increased significantly, and lumbar kyphotic sagittal angle (L-P SA) did not change significantly

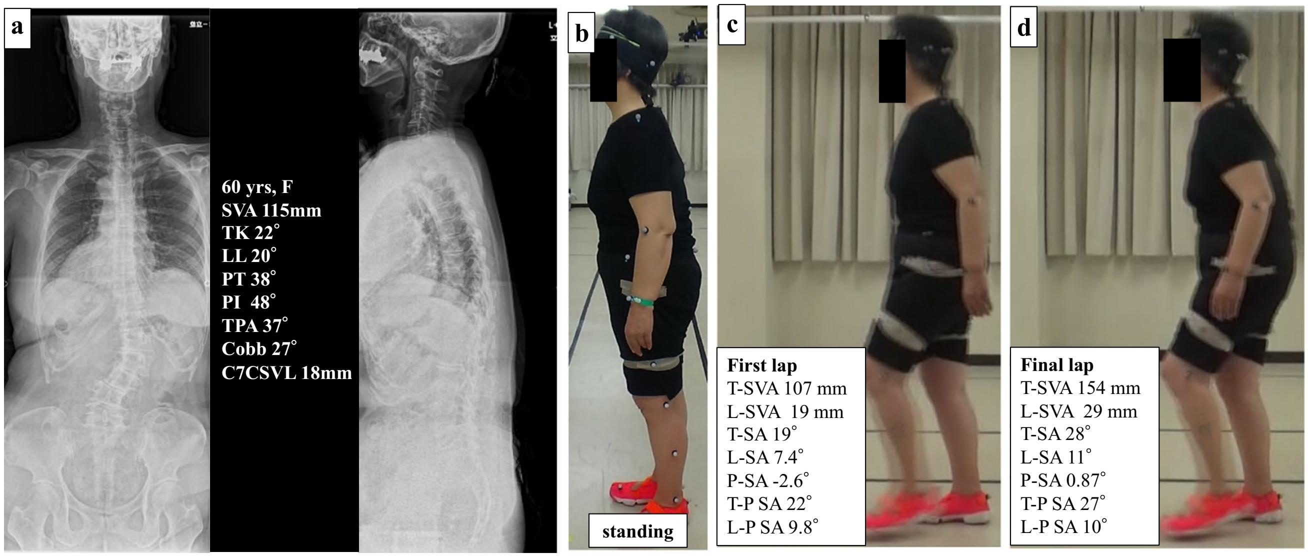

Fig. 6 An example of typical sagittal spinal balance change while walking. **a** Whole-spine radiograph with the patient in a standing position showing typical degenerative lumbar kyphoscoliosis. **b** Lateral posture on standing. **c** Lateral posture during 3D gait motion analysis at the first lap (Movie 1). **d** Lateral posture during 3D gait motion analysis at the final lap showing the increase of thoracic kyphosis and pelvic anteversion (Movie 2)

Table 3 Dynamic spinal parameters of sagittal balance (mean ± SD)

	First	Final	*P*
T-SVA (mm)	154 ± 51.5	172 ± 54.3	< 0.0001
L-SVA (mm)	24.1 ± 29.2	30.2 ± 32.8	0.01
S-SVA (mm)	201 ± 71.5	231 ± 78.9	0.0003
T-SA (°)	34.4 ± 14.1	39.2 ± 15.9	0.0005
L-SA (°)	9.70 ± 12.3	12.2 ± 13.6	0.006
S-SA (°)	27.0 ± 11.4	31.4 ± 13.2	0.0003
P-SA (°)	3.20 ± 7.46	5.18 ± 8.62	0.01
T-P SA (°)	30.5 ± 13.8	33.7 ± 13.6	< 0.0001
L-P SA (°)	6.38 ± 11.6	6.78 ± 11.0	0.21
S-P SA (°)	23.4 ± 11.6	26.0 ± 11.2	< 0.0001

Thoracic [T-], Lumbar [L-], Whole spine [S-]. SVA sagittal vertical axis, SA sagittal angle. [spinal segment]-SA is sagittal trunk tilt to vertical axis. P-SA is pelvic sagittal tilt to horizontal axis. [spinal segment]-P SA is sagittal trunk tilt to pelvic tilt

However, maintaining that compensation requires substantial muscle activity compared with that involved in normal spinal alignment [17–19]. Compensatory mechanisms are ultimately unable to maintain the gravity line position and horizontal gaze because of progression of deformity or inadequate muscle strength or endurance as a result of aging. Lamartina et al. defined this situation as uncompensated imbalance [19]. The present dynamic evaluation using 3D motion analysis demonstrated that thoracic kyphosis and pelvic anteversion increased while walking. These findings indicated that the compensation that decreased thoracic kyphosis and tilt pelvic retroversion could not be maintained after patients walked until they were fatigued. The static spinal parameters evaluated to define global sagittal misalignment were not significantly correlated with the increase of thoracic kyphosis. It is probably impractical to detect this failure of compensation by static evaluation using conventional whole-spine radiographs. Moreover, short-distance gait motion analysis may not detect its occurrence. We consider that for satisfactory analysis is it important to have the patient walk until a failure of the compensation occurs. We could detect the failure in compensation using the 3D motion analysis of continuous walking to the limit of the patient's endurance.

Recent technical progress in motion capture analysis enables us to detect dynamic spinal balance in detail. There are a few previous studies of dynamic spinal alignment changes during gait using a 3D motion analysis of patients with ASD. Shiba et al. revealed significant differences between dynamic and static parameters of global sagittal alignment in patients with degenerative lumbar kyphoscoliosis. Dynamic global sagittal alignment while walking was significantly worse than when the patients were standing still. Compensated nonergonomic global sagittal alignment while standing still was no longer maintained after walking commenced because compensatory mechanisms such as retroversion of the pelvis are ineffective while walking [14]. Sasaki et al. reported gait motion analysis in combination with a 3D musculoskeletal model produced from whole-body computed tomography and magnetic resonance imaging. Dynamic data while walking obtained from Vicon were input into the 3D musculoskeletal model, so that dynamic changes of the parameters of sagittal alignment for the spine and pelvis could be calculated. They found pelvic retroversion in elderly women decreased after they began walking [15]. Lee et al. evaluated characteristics of static and dynamic parameters in patients with a degenerative flatback to compare the degree of improvement between groups of patients with successful and unsuccessful surgical outcomes. They reported that surgical outcomes determined by the patients' satisfaction were more closely related to improvement in the dynamic parameters than improvement in static parameters [20].

The present study determined dynamic spinal balance quantitatively by 3D gait motion analysis. A methodological characteristic of our 3D gait motion analysis was continuous walking for as long as possible on flat ground. No significant change was observed in coronal spinal balance during walking.

By contrast, thoracic kyphosis and pelvic anteversion in the sagittal plane were increased by continuous walking. These dynamic changes indicated a failure of compensation presenting as a decrease of thoracic kyphosis and pelvic retroversion, which functioned only in temporary situations such as while standing. The static evaluation using conventional whole-spine radiograph and gait analysis of walking short distances might not be able to detect this failure. Thus, determining dynamic spinal balance using 3D gait motion analysis of walking to a patient's limit of endurance could lead to better understanding of the pathophysiology of each patient with adult spinal deformity. The 3D motion analysis does not require radiation exposure, and the 3D motion analysis system is convenient and can be easily disseminated because there is no need for special techniques to obtain data to analyze gait. Elucidating the compensatory failure of each patient with ASD has the potential to determine corrective surgical strategies such as the fusion level, resulting in better clinical outcomes.

There are several limitations to the present study. Primarily, the association between dynamic spinal balance obtained by 3D gait motion analysis and clinical symptoms such as low back pain and health-related quality of life was not evaluated. Compensatory failure might be related to muscle strength and endurance, so muscle strength and activity should be determined for a more complete picture of the compensatory failure. The accuracy of placing reflective markers on the skin should be taken into consideration. Schmid et al. reported that the placement of reflective markers on the lumbar spine was less accurate than it is on the thoracic spine because of the soft tissue thickness resulting from lumbar lordosis [21]. However, the influence on accuracy by soft tissue thickness is likely less than that found by Schmid et al. because of the decreased lumbar lordosis of patients in the present study. Nevertheless, in the 3D motion analyses, the influence of soft tissue on the accuracy of marker placement should be considered.

Conclusions

In addition to static analysis of spinal alignment using conventional whole spinal radiographs, 3D gait motion analysis can be used to elucidate the dynamic change of spinal balance in patients with ASD potentially leading to a better understanding of the pathophysiology of each patient. The 3D gait motion analysis of patients with ASD found that lumbar sagittal balance did not change significantly; by contrast, thoracic kyphosis and pelvic anteversion increased significantly while walking. These dynamic changes are considered to result from the ultimate failure of compensation for the spinal deformity. Identified pathophysiology may suggest appropriate corrective surgery, for example, by indicating fusion levels, thereby improving clinical outcomes.

Compliance with ethical standards

Conflict of interest The authors declare that they have no conflict of interest.

References

1. Glassman SD, Bridwell K, Dimar JR et al (2005) The impact of positive sagittal balance in adult spinal deformity. Spine (Phila Pa 1976) 30:2024–2029
2. Glassman SD, Berven S, Bridwell K et al (2005) Correlation of radiographic parameters and clinical symptoms in adult scoliosis. Spine (Phila Pa 1976) 30:682–688
3. Lafage V, Schwab F, Patel A et al (2009) Pelvic tilt and truncal inclination: two key radiographic parameters in the setting of adults with spinal deformity. Spine (Phila Pa 1976) 34:E599–E606. https://doi.org/10.1097/brs.1090b1013e3181aad1219
4. Mac-Thiong JM, Transfeldt EE, Mehbod AA et al (2009) Can c7 plumbline and gravity line predict health related quality of life in adult scoliosis? Spine (Phila Pa 1976) 34:E519–E527. https://doi.org/10.1097/brs.1090b1013e3181a1099c1097ad
5. Schwab F, Patel A, Ungar B et al (2010) Adult spinal deformity-postoperative standing imbalance: how much can you tolerate? An overview of key parameters in assessing alignment and planning corrective surgery. Spine (Phila Pa 1976) 35:2224–2231. https://doi.org/10.1097/brs.0b013e3181ee6bd4
6. Schwab F, Ungar B, Blondel B et al (2012) Scoliosis Research Society-Schwab adult spinal deformity classification: a validation study. Spine (Phila Pa 1976) 37:1077–1082. https://doi.org/10.1097/brs.0b013e31823e15e2
7. Lamartina C, Berjano P, Petruzzi M et al (2012) Criteria to restore the sagittal balance in deformity and degenerative spondylolisthesis. Eur Spine J 21:S27–S31. https://doi.org/10.1007/s00586-012-2236-9
8. Hasegawa K, Okamoto M, Hatsushikano S et al (2016) Normative values of spino-pelvic sagittal alignment, balance, age, and health-related quality of life in a cohort of healthy adult subjects. Eur Spine J 25:3675–3686
9. Obeid I, Boissiere L, Yilgor C et al (2016) Global tilt: a single parameter incorporating spinal and pelvic sagittal parameters and least affected by patient positioning. Eur Spine J 25:3644–3649

10. Miura K, Kadone H, Koda M et al (2018) Visualization of walking speed variation-induced synchronized dynamic changes in lower limb joint angles and activity of trunk and lower limb muscles with a newly developed gait analysis system. J Orthop Surg (Hong Kong) 26:2309499018806688. https://doi.org/10.1177/2309499018806688
11. Miura K, Kadone H, Koda M et al (2018) Three-dimensional gait analysis reveals dynamic alignment change in a patient with dropped head syndrome: a case report. J Clin Neurosci 48:106–108. https://doi.org/10.1016/j.jocn.2017.10.075
12. Miura K, Koda M, Kadone H et al (2018) Successful detection of postoperative improvement of dynamic sagittal balance with a newly developed three-dimensional gait motion analysis system in a patient with iatrogenic flatback syndrome: a case report. J Clin Neurosci 53:241–243. https://doi.org/10.1016/j.jocn.2018.04.051
13. Haddas R, Belanger T (2017) Clinical gait analysis on a patient undergoing surgical correction of kyphosis from severe ankylosing spondylitis. Int J Spine Surg 11:18. https://doi.org/10.14444/4018
14. Shiba Y, Taneichi H, Inami S et al (2016) Dynamic global sagittal alignment evaluated by three-dimensional gait analysis in patients with degenerative lumbar kyphoscoliosis. Eur Spine J 25:2572–2579. https://doi.org/10.1007/s00586-016-4648-4
15. Sasaki K, Hongo M, Miyakoshi N et al (2017) Evaluation of sagittal spine-pelvis-lower limb alignment in elderly women with pelvic retroversion while standing and walking using a three-dimensional musculoskeletal model. Asian Spine J 11:562–569. https://doi.org/10.4184/asj.2017.11.4.562
16. Van Royen BJ, Toussaint HM, Kingma I et al (1998) Accuracy of the sagittal vertical axis in a standing lateral radiograph as a measurement of balance in spinal deformities. Eur Spine J 7:408–412
17. Barrey C, Roussouly P, Perrin G et al (2011) Sagittal balance disorders in severe degenerative spine. Can we identify the compensatory mechanisms? Eur Spine J 20:626–633. https://doi.org/10.1007/s00586-011-1930-3
18. Le Huec JC, Charosky S, Barrey C et al (2011) Sagittal imbalance cascade for simple degenerative spine and consequences: algorithm of decision for appropriate treatment. Eur Spine J 20:699–703. https://doi.org/10.1007/s00586-011-1938-8
19. Lamartina C, Berjano P (2014) Classification of sagittal imbalance based on spinal alignment and compensatory mechanisms. Eur Spine J 23:1177–1189. https://doi.org/10.1007/s00586-014-3227-9
20. Lee JH, Lee SH (2016) Static and dynamic parameters in patients with degenerative flat back and change after corrective fusion surgery. Ann Rehabil Med 40:682–691. https://doi.org/10.5535/arm.2016.40.4.682
21. Schmid S, Studer D, Hasler CC et al (2015) Using skin markers for spinal curvature quantification in main thoracic adolescent idiopathic scoliosis: an explorative radiographic study. PLoS ONE 10:e0135689. https://doi.org/10.1371/journal.pone.0135689

Publisher's Note Springer Nature remains neutral with regard to jurisdictional claims in published maps and institutional affiliations.

Affiliations

Kousei Miura[1,2] · Hideki Kadone[3] · Masao Koda[1] · Tetsuya Abe[1] · Toru Funayama[1] · Hiroshi Noguchi[1] · Kentaro Mataki[1] · Katsuya Nagashima[1] · Hiroshi Kumagai[1] · Yosuke Shibao[1] · Kenji Suzuki[4] · Masashi Yamazaki[1]

✉ Kousei Miura
kmiura@tsukuba-seikei.jp

[1] Department of Orthopaedic Surgery, Faculty of Medicine, University of Tsukuba, 1-1-1 Tennodai, Tsukuba, Ibaraki 305-8575, Japan

[2] Department of Rehabilitation Medicine, Faculty of Medicine, University of Tsukuba Hospital, 1-1-1 Tennodai, Tsukuba, Ibaraki 305-8575, Japan

[3] Center for Innovative Medicine and Engineering, University of Tsukuba Hospital, 1-1-1 Tennodai, Tsukuba, Ibaraki 305-8575, Japan

[4] Center for Cybernics Research, University of Tsukuba, 1-1-1 Tennodai, Tsukuba, Ibaraki 305-8575, Japan